MICROFLUIDICS BASED NEURONAL AGGREGATE CULTURING DEVICE FOR HIGH THROUGHPUT DRUG SCREENING

A Thesis

by

JOHN EDWARD BUONOCORE

Submitted to the Office of Graduate and Professional Studies of
Texas A&M University
in partial fulfillment of the requirements for the degree of

MASTER OF SCIENCE

Chair of Committee,	Arum Han
Co-Chair of Committee,	Jianrong Li
Committee Members,	Jim Ji
	Jun Kameoka
Head of Department,	Miroslav Begovic

May 2017

Major Subject: Electrical Engineering

ABSTRACT

Neurodegenerative diseases are extremely debilitating and affect a large portion of the population. Quality care for diseases such as multiple sclerosis relies heavily on the development of therapeutic agents by pharmaceutical companies. Currently neuronal drug development processes are time consuming and costly. This has led to a lack of commercially available drugs targeted at the nervous system. This thesis presents a novel neuronal cell microfluidic chip in response to this problem. In many neurodegenerative diseases, demyelination of the axons plays a critical role. This thesis presents a novel way to improve the efficiency of a neuronal cell aggregate device for myelination studies. The device is fabricated using traditional lithography techniques to pattern three inch SU-8 wafers. These wafers are then used as the master molds for the fabrication of polydimethylsiloxane (PDMS) devices. The device incorporates multiple normally closed micro valves. Fabrication of neuronal aggregate trapping structures is necessary and required the use of Inductively Coupled Plasma (ICP) to etch trenches in silicon. Neuronal aggregates are loaded into the device and trapped in a specific culturing chamber by pillar trapping structures. Unused aggregates are reflowed through the device until all the aggregate trapping sites are full. The aggregates are then cultured for multiple weeks. During culturing, myelin is produced by the aggregates. The goal of the device is to enhance drug testing related to the myelination of neurons and limit the need of animal models for such drug testing. This thesis focuses on the creation of a device

that is able to reflow the unused neuronal aggregates back through the trapping chambers.

DEDICATION

I dedicate this thesis to my family, especially my grandmother. I also dedicate this thesis to the furthering of scientific knowledge in the area of study related to neurodegenerative diseases. May the cure for neurodegenerative diseases be quickly found.

ACKNOWLEDGEMENTS

I would first like to thank my mentor Sehoon Jeong for his guidance and patience in the training process.

I would like to thank my committee chair, Dr. Han, and my committee members, Dr. Li, Dr. Ji, and Dr. Kameoka, for their guidance and support throughout the course of this research.

Thanks also go to my friends and colleagues and the department faculty and staff for making my time at Texas A&M University a great experience.

Finally, thanks to my mother and father for their encouragement.

CONTRIBUTORS AND FUNDING SOURCES

Contributors

This work was supervised by a thesis committee consisting of Professor Arum Han [advisor], Professor Jim Ji and Professor Jun Kameoka of the Department of Electrical Engineering and Professor Jianrong Li of the Department of Veterinary Studies.

All work for the thesis was completed by the student, under the advisement of Dr. Arum Han of the Department of Electrical Engineering.

Funding Sources

This work was made possible in part by the National Institute of Health (NIH) under Grant Number #1R21EB021005

Its contents are solely the responsibility of the authors and do not necessarily represent the official views of the National Institute of Health.

NOMENCLATURE

ICP	Inductively Coupled Plasma
PDMS	Polydimethylsiloxane
RIE	Reactive Ion Etching

TABLE OF CONTENTS

Page

LIST OF FIGURES

Page

LIST OF TABLES

Page

CHAPTER I

INTRODUCTION AND LITERATURE REVIEW

1.1 Myelination and Demyelinating Diseases

Over 2.3 million people are affected with multiple sclerosis worldwide according to the National Multiple Sclerosis Society. Many more are affected with dementias such as Alzheimer's disease. What links these diseases is not only that they attack the neurological system, but that they result in the demyelination of neurons.

Myelin is a fatty substance that surrounds neuronal axons. It is produced by Schwann cells in the peripheral nervous system and by oligodendrocyte cells in the central nervous system. The importance of myelin resides in the fact that it increases the speed of the electrical signal flowing along the axon. Myelin insulates the axon, improving the speed of signal transmission. More specifically, myelin ensures membrane depolarization occurs only at the nodes of Ranvier as shown in Figure 1.

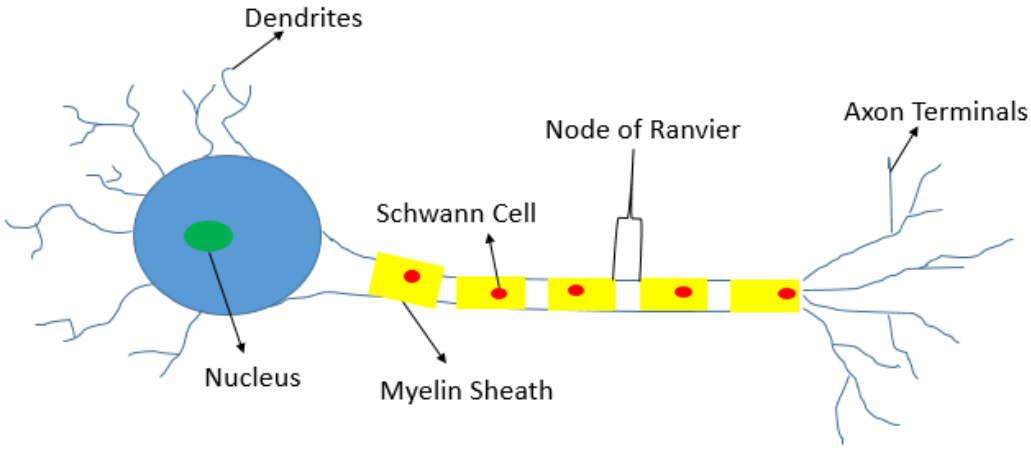

Figure 1: Neuron cell

Such controlled depolarization of the axons allows for signal propagation [6]. Without the myelin sheath in Figure 2, the transmission of the ion cascade along the axon is too slow for the brain to send or receive messages. This results in impaired motor control and degradation of neuronal pathways. A significant amount of research focuses on studying and understanding ways to prevent demyelination as well as repair damaged myelin.

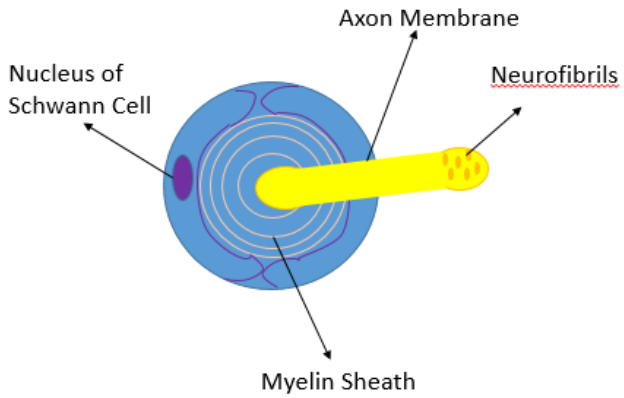

Figure 2: Myelination of neurons with surrounding Schwann cells

Much of this research focuses on discovering the mechanisms behind severely debilitating dementias such as Alzheimer's disease. Alzheimer's disease attacks the white matter of the brain (WM) resulting in lesion formation in the WM. Luxol fast blue (LFB) staining of myelin in the WM of those who suffered from dementing disorders showed significantly increased myelin loss in the frontal lobe [5]. Research into the mechanisms behind this myelin loss as well as the mechanisms behind myelin development are underway. Determining why some axons are myelinated and some are not is still unknown and highlights the need for increased research [6]. The thickness of myelin on the axon also plays an important role in proper functioning of the axon. Myelin thickness is typically measured using the g-ratio (axonal diameter/axonal diameter and myelin sheath). This ratio is usually the same for different axons in animals. Therefore, larger axons normally have a larger myelin sheath [6]. Discovering signaling molecules that affect the development and thickness of the myelin sheath is a

focal point of research. Currently, the ErbB3 receptor system is believed to affect the thickness of myelination of neurons [6]. Disruption of this receptor affects the Schwann cells surrounding the axon. Adjusting the ErbB3 receptor system may result in a possible therapy for dementias. Another possibly therapeutic treatment for Alzheimer's and other demyelinating diseases are Rho kinases (ROCKS). Rho kinases were shown in 2005 to inhibit regeneration of neuronal tissue. Conversely, inhibition of ROCKS shows increased neuron regeneration in damaged tissue [10]. This includes regeneration of tissue damaged by diseases such as Alzheimer's and other dementias. Developing inhibitors of ROCKS will increase the regeneration of damaged neural tissue. Despite the promising outlook for such a therapeutic, ROCKS inhibitors are still undergoing clinical trials with the FDA.

Another disease that would be affected by inhibition of rho kinases is Multiple Sclerosis (MS). Signaling pathways play an important role in the onset of MS. MS affects the ability of axons to remyelinate. Fibroblast growth factor 9 (FGF9) has been shown to prevent myelination and remyelination of axons. Excessive amounts of FGF9 indirectly affect oligodendrocyte cells. The mechanism has been linked to secretions by astrocyte cells surrounding the oligodendrocyte cells [7]. Inhibition of the FGF signaling pathway in astrocyte cells may serve as a therapeutic treatment that would increase remyelination of neurons in patients with MS [7]. Another potentially related therapy for MS is the regulation of the astrocyte response to increased immune activity. Astrocytes, one of the cells that support neurons, play a significant role in the demyelination of axons in patients with MS. During an increased immune response,

astrocytes breakdown the myelin sheath. MS is an autoimmune disease and results in an immune response against neuronal cells and the myelin surrounding the axons. Astrocytes contribute to the immune response by breaking down the myelin sheath [8]. Regulating the uptake of myelin by astrocytes may serve as a potential treatment for the slowing of demyelination as a result of MS [8].

Despite such innovative research, current MS therapeutic treatments still rely on suppression of the immune system. New oral medications such as Fingolimod work by reducing the amount of white blood cells that enter the central nervous system (CNS) [9]. Such therapeutics only indirectly treat MS. A similar problem occurs for medications targeting various dementias. As previously mentioned, new potentially revolutionary drugs such as ROCKS inhibitors have yet to become commercially available. Current therapeutics available for the treatment of dementia only slow the disease. The lack of suitable commercially available drugs for neurodegenerative diseases is apparent and results from multiple factors.

One of the factors is the increased cost and complexity of developing drugs targeted at the nervous system. Drugs targeted at the nervous system have a 95% rate of failure and take 10-15 years to move from conceptualization to commercialization [11]. A prime example is the number of drugs related to Alzheimer's disease. The number of drug failures for Alzheimer's disease has been estimated at 101 since 1998 as compared to 3 successes [11]. Such high failure rates affect the number of neurologically related drugs that pharmaceutical companies are willing to invest in. In a recent report published by Tufts University, a total amount of $2.6 billion was said to have been spent on

average to produce a new pharmaceutical drug [12]. The study was based on information obtained from 10 unnamed drug makers. Of the $2.6 billion, almost half or approximately $1.2 billion was ascribed to capital lost due to potential drug failure [12]. This amount is even higher for drugs targeted at the nervous system. The amount of time the drug companies spend researching a drug that fails is counted as a cost in the development of a new successful drug. The remaining $1.4 billion is spent on actual research for the drug [12]. Reducing the cost of research will reduce the cost of failure. Having a cost effective way to test possible neurological drug candidates will increase the efficiency and decrease the cost of drugs targeted at the nervous system.

Traditionally, pharmaceutical companies are required to perform multiple *in vivo* animal studies before beginning clinical trials. These animal studies are necessary. However, they add greatly to the cost of drug production. The creation of a high throughput device that enables pharmaceutical companies to test different drug concentrations before initiating animal testing will greatly reduce the cost of drug development by limiting the number of animal trials. Having a cheaper alternative to animal testing will limit the cost of failure by providing prescreening of potential drug candidates. A high throughput screening platform for neurological drug candidates allows a large number of potential candidates to be tested in a relatively cheap manner. Only the drug candidates that are successful will move on to more expensive animal testing. The requirements for such a high throughput system are that it simulates the *in vivo* environment and is cost effective. While it is challenging to mimic the *in vivo*

environment and maintain a cost effective platform, modern microfluidics has led to such breakthroughs.

1.2 Micro Devices for Neuron Cell Culture

Microfluidic devices play a large role in the creation of suitable *in vitro* environments for cell culturing. In contrast to standard petri dish cultures, fluidic devices enable modification of the cellular environment from culturing cells on membranes, to generating 3D cell cultures within integrated microfluidic systems [2, 22, 24]. Microfluidics allow for precise handling of small amounts of fluid as well as laminar fluid flow due to the small fluid volumes [22]. Through the use of membrane valves, microfluidic designs are able to precisely regulate fluid within microchannels [22, 26]. Automation of membrane valves enable the production of large integrated microfluidic designs [22, 23].

Two major types of microfluidic valves are normally open and normally closed valves. Normally open valve require pressure to be applied to close the valve. Normally closed valves require negative pressure to open the valve layer.

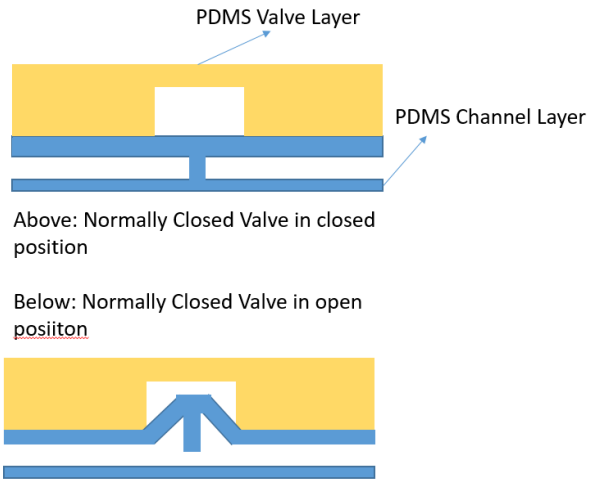

Figure 3: Normally closed valve design

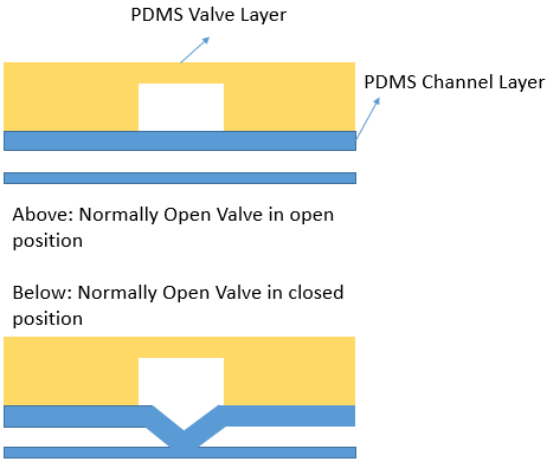

Figure 4: Normally open valve design

Negative pressure is applied to the PDMS valve layer in the case of the normally closed valve shown in Figure 3. This results in the popping up of the top part of the PDMS channel layer, which opens the valve to flow. Positive pressure is applied in the case of

the normally open valve in Figure 4 which results in the pushing down of the top part of the microfluidic channel layer, closing the channel to flow. Using the basic operating principles of the above designs, microfluidic large scale integration (mLSI) is possible [27]. Microfluidic large scale integration is the incorporation of multiple microfluidic valves for the automation of biological and chemical processes [27]. Such large scale integration is crucial for the development of high throughput microfluidic devices. The development of the microfluidic valve is analogous to the development of the transistor in the semiconductor industry. Increasing the valve density per microfluidic chip as well as the response time of the valves are key areas of research [27]. Multiple types of valves including heat sensitive resistive valves have been developed [27]. Within this work, we will rely on the traditional microfluidic valve designs fabricated through soft lithography methods and depicted in the above figures. Specifically, normally closed valves following the operation shown above, have been fabricated.

Due to their miniaturized design, fluidic devices also provide for high throughput screening and testing. Parallelization of different processes on a single device allows for increased throughput [22]. High throughput screening (HTS) is a term used to describe the pharmaceutical industry's drug testing process [2]. Through automation, multiple drug candidates are tested and their viability is measured. This system endeavors to be a low cost way to screen multiple experimental drugs. Various Lab-on-a-Chip and Organ-on-a-Chip devices are fabricated in an attempt to harness these desirable characteristics of microfluidic devices.

Lab-on-a-Chip and Organ-on-a-Chip microfluidic devices are used in the characterization and culture of many different types of cells. The versatility of the design process for microfluidic devices enables the creation of a tailored cellular environment [24]. Liver cell cultures were one of the first cells to be cultured on a microfluidic device [2]. The need to culture liver cells in an environment that mimicked *in vivo* conditions was necessary to provide better drug testing [2].

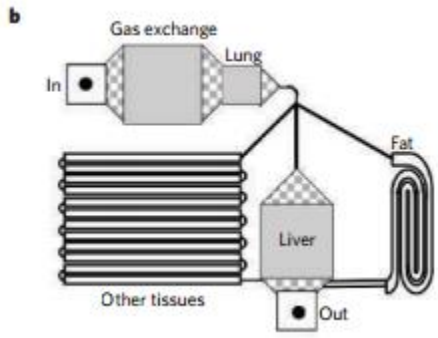

Figure 5: Example of early organ-on-a-chip culturing device. [2]

In the above Figure 5, a cellular culturing device was fabricated using traditional microfluidic techniques and cultured liver and lung cells. The liver and lung areas of the chip provided the culturing sites for the cells. The gas and fat areas provided for *in vivo* like stimuli to influence cell growth and adaptation.

Cellular microsystems have grown from the original liver on chip devices to even more advanced microfluidic devices. Devices have been customized to each particular cell type to provide the best environment for cellular growth [24]. Numerous

microfluidic devices have been tailored to the culturing of neuronal cells. Some of the earliest neuronal cell culturing systems include the use of biomarkers and cell guidance [1]. Microfluidic neuronal cell culture systems are used to study the cues relating to axon guidance. This is crucial for the study of brain development and function. One way of tracking the growth of axons is by immobilizing proteins on the channel surfaces of the device. Culturing of cells for neuronal devices is often done in a larger area off chip. The mature neuronal cells are then delivered to the chip [1, 25].

In Hong Yang, a leading researcher in neuroengineering, has developed a microfluidic platform that provides electrical stimulation to growing axons.

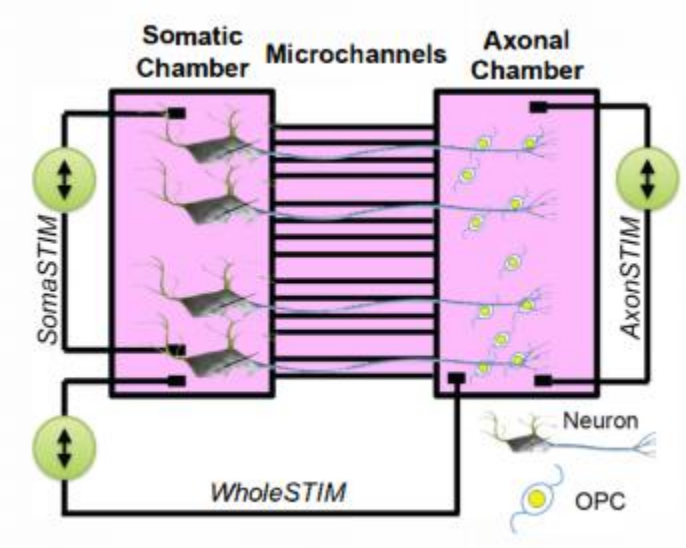

Figure 6: Microfluidic device for electrical stimulation of neuronal axons. [13]

The device in Figure 6 incorporates two separate culturing chambers connected by a series of thin channels. This two chamber design has previously been used for neuronal research by Jeong Won Park et al [17]. Building from his design, Jean Michel Peyrin et al adjusted the widths and shapes of the channels connecting the somatic and axonal cell culturing chambers [19]. Such a two chamber design became the fundamental neuronal cell culturing microfluidic design. Yiing C. Yap et al incorporated such a design to test the response of neuronal cells to axon injury [18]. The novelty of such a design lies in the ability to structurally separate the axons from the neuronal cell body. Regarding the above figure, primary dorsal root ganglion cells (DRGs) were plated in the somatic chamber and their axons grew through the microchannels into the axonal chamber. Separation of the cell bodies with the axons allowed for independent testing of the neuronal cell bodies and the axons. Electrical stimulation was applied across the microchannels with electrodes positioned in each of the culturing chambers. Due to the high impedance within the microchannels, only the neurons with axons protruding through the microchannels received electrical stimulation. Oligodendrocyte progenitor cells (OPCs) were cultured in the axonal chamber. Oligodendrocytes were added to produce myelin sheaths around the axons. Results found that electrical stimulation resulted in increased maturation of the OPCs and increased myelination of the axons [13]. Maturation of the OPCs led to oligodendrocyte production of myelin. Such a device will be used to study the separate functioning of the axons and the cell body and how they sometimes operate independently from each other [13].

A similar device was developed by Eun-Mi Hur in collaboration with In Hong Yang to study the effects of chemotherapy on neuronal cells. The microfluidic device followed a similar design as the device previously described. It contained two neuronal cell culturing chambers, one for the main cell body and one for the axonal cell body. Application of a chemotherapeutic agent to the axonal and neuronal culturing chambers showed an increased detrimental effect on the axons [14]. Such a microfluidic system is used to study axonal degeneration which may include demyelination in future studies [14]. This microfluidic chip design consisting of two compartmentalized culture chambers was further used to study the effects of regenerative axonal growth [15]. Using a similar design, the neuronal growth cone, at the tip of each axon, was modified. The microtubules that attach to the growth cone were altered and this changed the shape of the cytoskeleton [15]. Such alterations increased the regeneration of axons from previously damaged neuronal cells [15].

One of the drawbacks of the previously mentioned devices is the ability to load the neuronal cells into the somatic culturing chamber. This issue was addressed through the design of a circular somatic cell culturing chamber [25].

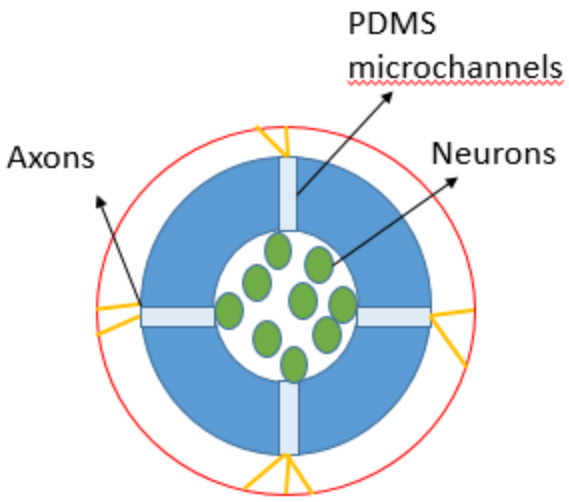

Figure 7: Circular neuronal aggregate device design. [25]

In Figure 7, the mature neuronal cells were loaded into the center chamber and axon formation occurred through the microchannels into the axon/glia compartment. Separation of the neuronal cell bodies from the corresponding axons was achieved as well as easy loading of the neuronal cells. Furthermore, oligodendrocyte cells (OLs) were successfully cultured in the axon/glia compartment [25]. These cells are primarily responsible for the formation of myelin sheaths around axons.

Application of an electrical stimulus to neuronal cells is useful for many reasons including the possibility of increased myelination [3]. The inclusion of a microelectrode array (MEA) into the design of a neuronal microfluidic chip poses many advantages for delivering electrical stimulus to neuronal cells. As shown in the paper by Fabrice Morin et al, a MEA was used to record the electrical signals from neuronal networks cultured

on a microfluidic platform [16]. Both commercially available MEAs and custom planar MEAs were incorporated into the microfluidic system. The custom planar MEAs, as shown in Figures 8 and 9, were fabricated on a glass substrate using standard microfabrication techniques.

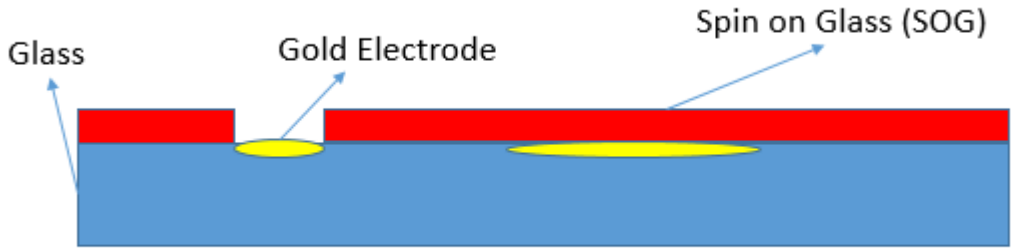

Figure 8: Custom planar MEA. [16]

Gold was used as the material for the electrodes. An intermediate chrome layer was used to bond the gold layer to the glass substrate. A spin-on-glass (SOG) layer was patterned to cover the gold wiring while allowing openings for the electrodes to interact with the neuronal cell culture.

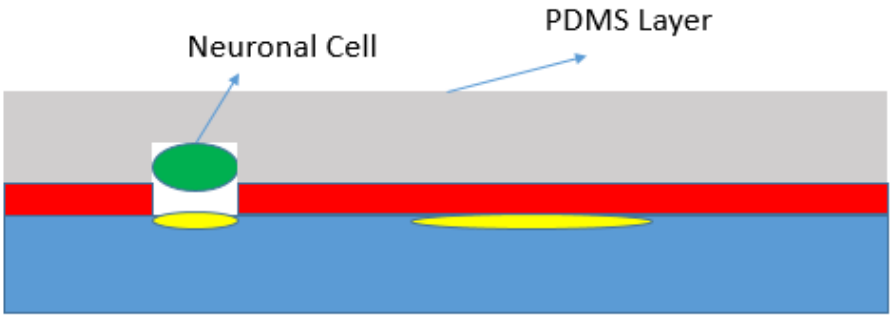

Figure 9: Added PDMS layer with microwells for neuronal cell culture. [16]

A layer of PDMS fabricated from an SU-8 mold was bonded to the MEAs. The neuronal cells were seeded ono the PDMS substrate and cultured. Their electrical signals were recorded for several weeks. This research demonstrated the ability to culture neuronal cells for long periods in microfluidic channels while simultaneously recording electrical stimulation. Electrical stimulation in the form of a biphasic square wave lasting a total of 10 ms was applied to the stimulating electrode. The response of the electrical response of the neuronal cells to the stimulation was measured [16].

The incorporation of electrical stimulation into neuronal cell cultures within a microfluidic platform opens a host of opportunities for insight into neuronal cell function as well as various drug testing. Attaching the previous microelectrode array to the PDMS substrate proved challenging [16]. To avoid this problem, a microfluidic platform containing liquid electrodes was utilized and is depicted in Figure 10 [20]. Gallium and eutectic gallium were chosen as the liquid metals for the electrodes. A PDMS device was fabricated using SU-8 patterned silicon wafers and plasma bonded to a glass slide.

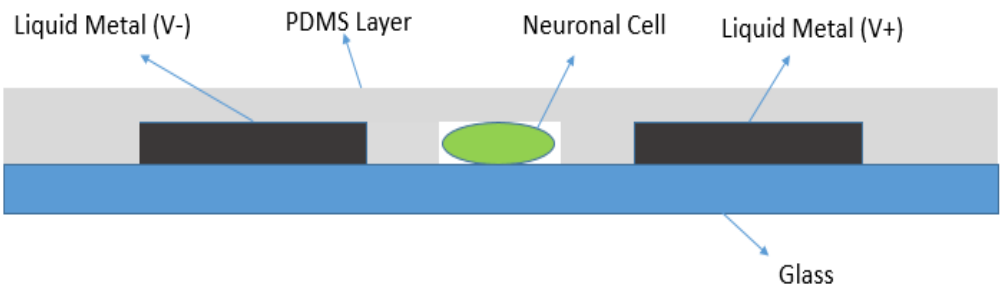

Figure 10: Electrical stimulation of neuronal cells. [20]

Two channels were patterned for the electrodes in the PDMS. These channels were filled with the liquid metal and used as the electrodes. A positive and negative voltage was applied to each of the liquid electrode channels. Hippocampal neurons were harvested from E17 rats for culture in the microchannels [20].

The biocompatibility of the liquid metal electrodes was assessed by comparing neuronal cell proliferation close to the electrodes (less than 3mm) to proliferation further away (greater than 3mm). The cell viability close to the electrodes was similar to the cellular viability in other parts of the chip [20]. Calcium indicator dye provided a visual indication of neuronal cell stimulation. The hippocampal neurons exhibited depolarization in response to electrical stimulation of 0.6 mA by the metal liquid electrodes. Successful stimulation of the neurons using the metal electrodes eliminates the costly fabrication of MEAs and the bonding process with the PDMS channel layer [20]. Furthermore, gallium is known for its low toxicity as a metal and is often used in glass thermometers in replace of mercury. Despite these promising attributes, current microfluidic designs have revolved around conventional electrodes. This is most likely

due to the difficulties of working with a liquid metal including the ability to attach wires to a liquid.

In addition to microfluidic designs, an organic transistor was developed for electrically stimulating neurons [21]. The motivation behind producing an organic field effect transistor (OFET) include the drawbacks to using traditional MEAs to measure neuronal activity. MEAs suffer from attachment issues between the electrodes and the cells. Furthermore, the electrode impedance of an MEA limits its size and measurement sensitivity. The OFET proposed by Valentina Benfenat et al, has increased biocompatibility for long term cellular recordings and provides bidirectional electrical stimulation of neurons. Bidirectional stimulation should increase the functionality and response of neurons to electrical stimuli. The results of the OFET were compared to electrical stimulation of neurons by MEAs. The OFET was found to have a higher signal to noise ratio than the MEA. Dorsal root ganglion (DRG) primary neuron cells were cultured for the experiment [21].

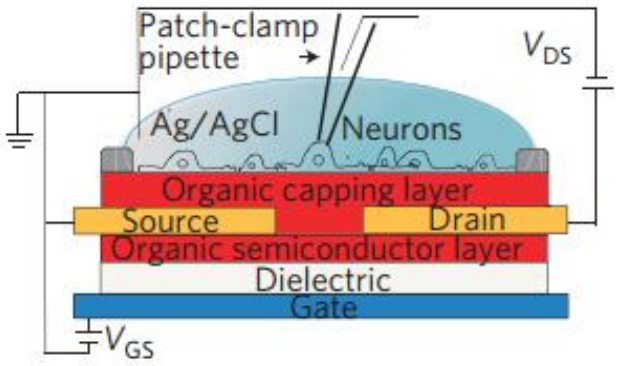

Figure 11: Organic Field Effect Transistor (OFET). [21]

The device in Figure 11 was manufactured using N,N0 - ditridecylperylene-3,4,9,10-tetracarboxylic diimide (P13) as the organic semiconductor layer. The intracellular membrane potential of the neuronal cells was determined through traditional patch clamp techniques. When a current was initiated between the source and drain regions, the intracellular potential was monitored to ensure electrical stimulation of the neurons [21]. Device characterization was carried out to ensure the transistor was working properly. Current saturation graphs were obtained for different drain and source voltages. Once the set up mimicked transistor properties, experimental tests were conducted to vary the electrical stimulation across the neuronal layer by varying the source to drain current [21]. While not explicitly a microfluidic device, the above design seeks to achieve electrical stimulation of neurons for the purpose of biological study as well as eventual pharmaceutical applications. Moving from a device as previously presented to a practical device for drug testing has drawbacks both in terms of size and relative complexity. Two major advantages of microfluidic designs continue to be the decreased size and lower cost.

The previously discussed electrical stimulation of neurons proves important in the study of neuron myelination. The development of a drug screening device to test drugs that affect the myelination of neurons requires the formation of neuron aggregates. *In vitro* cultured individual neurons don't produce myelin. Only groups of aggregated neurons form myelin sheaths. Therefore, in order to test the effects drugs have on myelin production, the first step is to form neuron aggregates. Neuron aggregates are formed in multiple ways. One way to form aggregates is to place individual neuron cells into a

poly dimethylenesiloxane (PDMS) tray with multiple microwells. The neuron cells attach to the surface of the tray and clump together in the micro wells. After a period of culturing, the clumps of neuron cells are removed from the microwells as aggregates.

These aggregates are then transferred to the neuronal aggregate microfluidic device. Once loaded onto the device, the aggregates are flown through multiple culturing chambers. Aggregate trapping structures will be implemented into these chambers to capture the neuronal aggregates. Various cell trapping techniques were considered for the trapping of the neuronal aggregates. The typical aggregate size varied from 150-200 um diameter spherical aggregates. Hydrodynamic traps as shown in the paper by Di Carlo follow the idea of allowing fluid flow through the trapping structure [28]. This is an important aspect of the neuronal aggregate trapping structure because the fluid flow through the trap leads to the trapping of the aggregate. Di Carlos employs hydrodynamic trapping to trap single HeLa cells, 20 um diameter, which are smaller in diameter than the aggregates [28]. Due to the size of the neuronal aggregates hydrodynamic trapping is not possible. Numerous other trapping techniques including dielectrophoresis (DEP) and magnetic trapping have been conducted within microfluidic devices [29]. DEP relies on generating a non-uniform electric field. Dielectric objects in the electric field experience a force that is used to move the objects into a trapping structure. These trapping techniques are effective however they increase the complexity of the system. For the longer term neuronal aggregate culture, a more practical aggregate trap exists [3]. The planned trapping structure for the aggregates is the previously fabricated three pillar design.

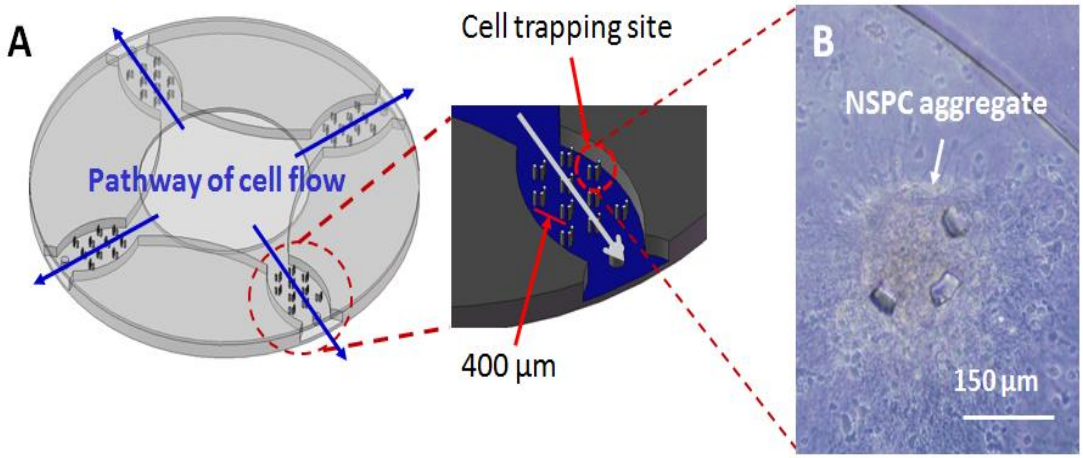

Figure 12: Previous microfluidic aggregate trapping design. [3]

Figure 12 shows the previous microfluidic device and trapping structures that were previously tested to study the myelination of neuronal aggregates. The goal of this thesis is to improve the throughput of the above design and minimize the aggregate losses during loading. Previously, the aggregates were pipetted into the center of the above design. They flowed into all four of the surrounding trapping chambers. A very high aggregate concentration was used during the loading step due to high aggregate loss. Furthermore, not all of the aggregate traps in each trapping chamber were filled upon loading of the aggregates. Empty trapping sites reduced the efficacy of the device. This thesis addresses the above issues by providing a recirculation of initially un-trapped aggregates.

In addition to providing a recirculation design, similar pillar trapping designs were investigated and preliminary fabrication work was done. In the previous device, the aggregates were cultured for a period of up to four weeks in order for myelination to occur. Once myelination is quantified in the aggregates, drug compounds can be tested on the aggregates. The difficulties with such a system include the manual process of loading and unloading neuronal aggregates once they are formed. Another inherent difficulty is the trapping of neuronal aggregates within culturing sites after unloading from a microwell. Automation of a complete neuron aggregate formation and culturing system is necessary for introduction of such a system into the pharmaceutical industry. The following proposal introduces steps to achieve a high throughput neuronal aggregate trapping and culturing device. The goals of the device are to increase the throughput of the previous neuron aggregate culturing device as well as reduce neuronal aggregate loss. To improve neuronal aggregate loss, the design focuses on the recirculation of neuronal aggregates within a microfluidic device.

CHAPTER II

NEURONAL AGGREGATE DEVICE

2.1 Design and Working Principle

A microfluidic device was fabricated to minimize neuronal aggregate loss for the previously mentioned myelination experiment. The device incorporates multiple microfluidic valves to reflow aggregates through the trapping chambers. Design constraints include the need to flow 200 um aggregates through the device. This necessitated designing the smallest channel to be at least 200 um height and 400 um width. Three input areas were incorporated into the device to prevent sticking of the aggregates along the edges of the channel during loading and for better control of the flow during cell loading. The recirculation of the free aggregates is performed through a series of steps. Each step involves the opening and closing of different microfluidic valves. The neuronal aggregates are first loaded into an initial reservoir chamber with an outlet channel. Once all the aggregates have been loaded into the initial reservoir chamber, the outlet chamber in the initial reservoir closes by action of a microfluidic valve. Next, a valve in the trapping chambers opens and the aggregates flow through the trapping chambers. The aggregates flow through the trapping chambers into the secondary reservoir. Once the aggregates move into the secondary reservoir, another microfluidic valve is opened and they flow back into the first reservoir where the process repeats until all trapping structures have been filled.

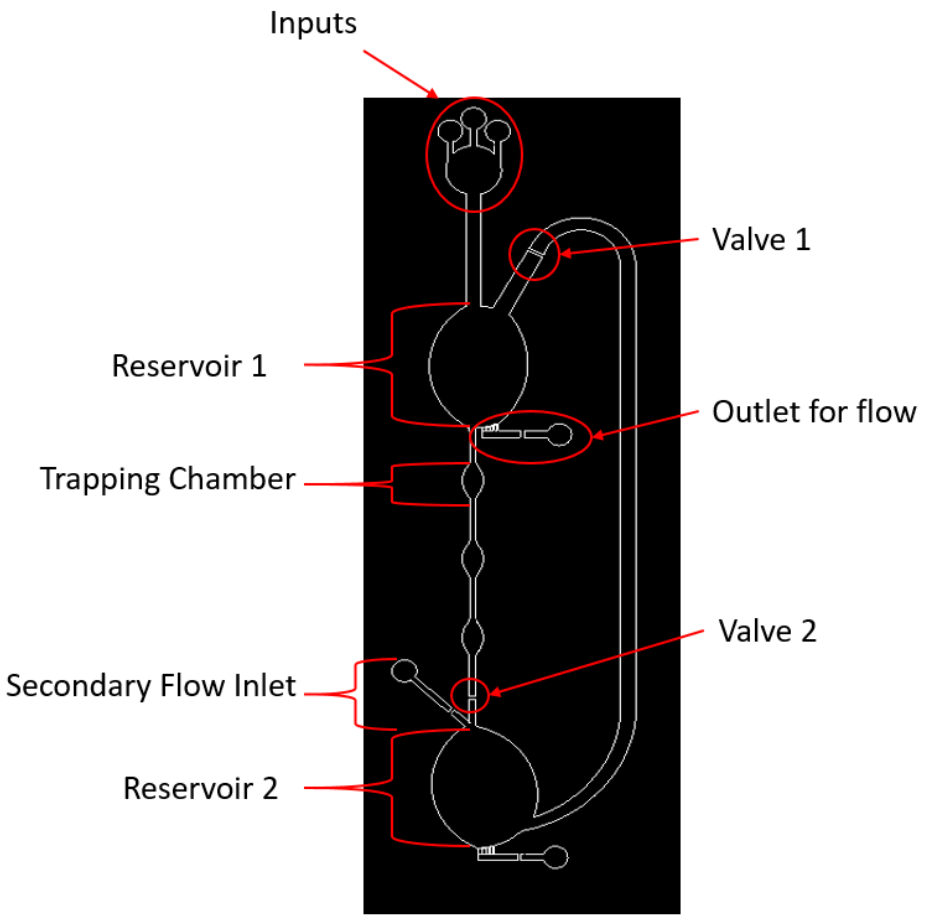

Figure 13: Reflow design

Currently, the design in Figure 13 incorporates three trapping chambers with no trapping structures. After proving reflow of the neuronal aggregates, the design will be fabricated to include the aggregate traps. The design will be expanded to include more trapping chambers.

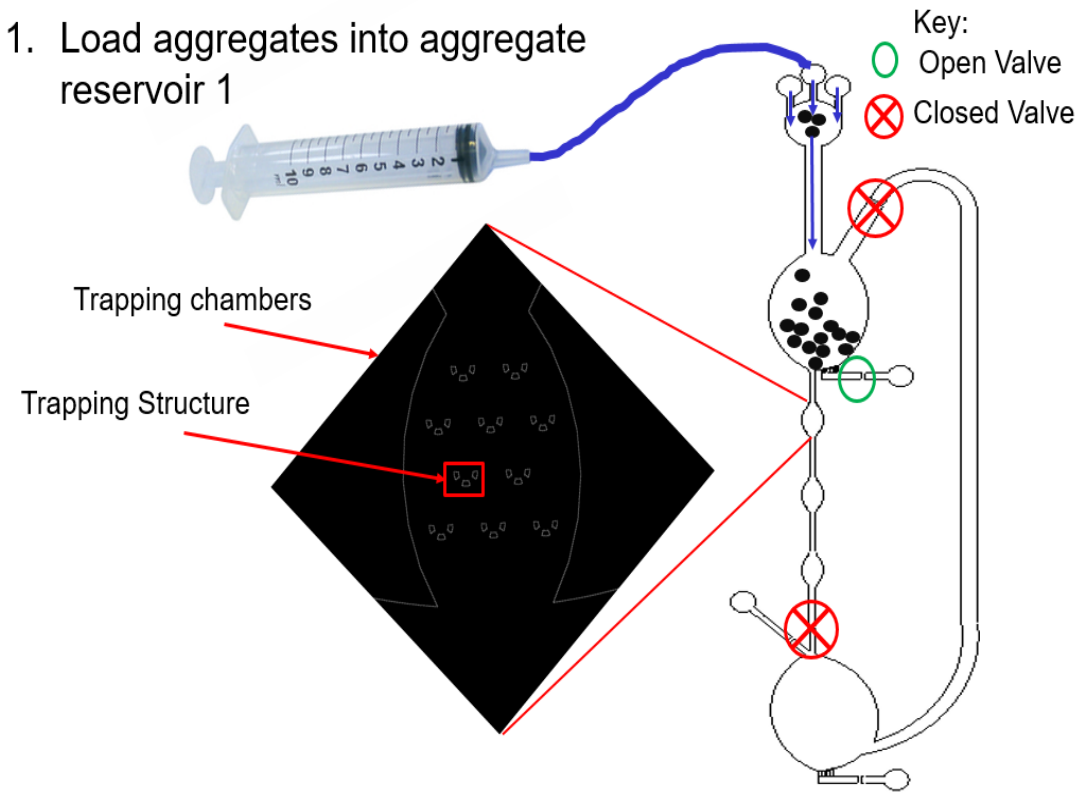

Figure 14: Step 1 is the loading process of the aggregates

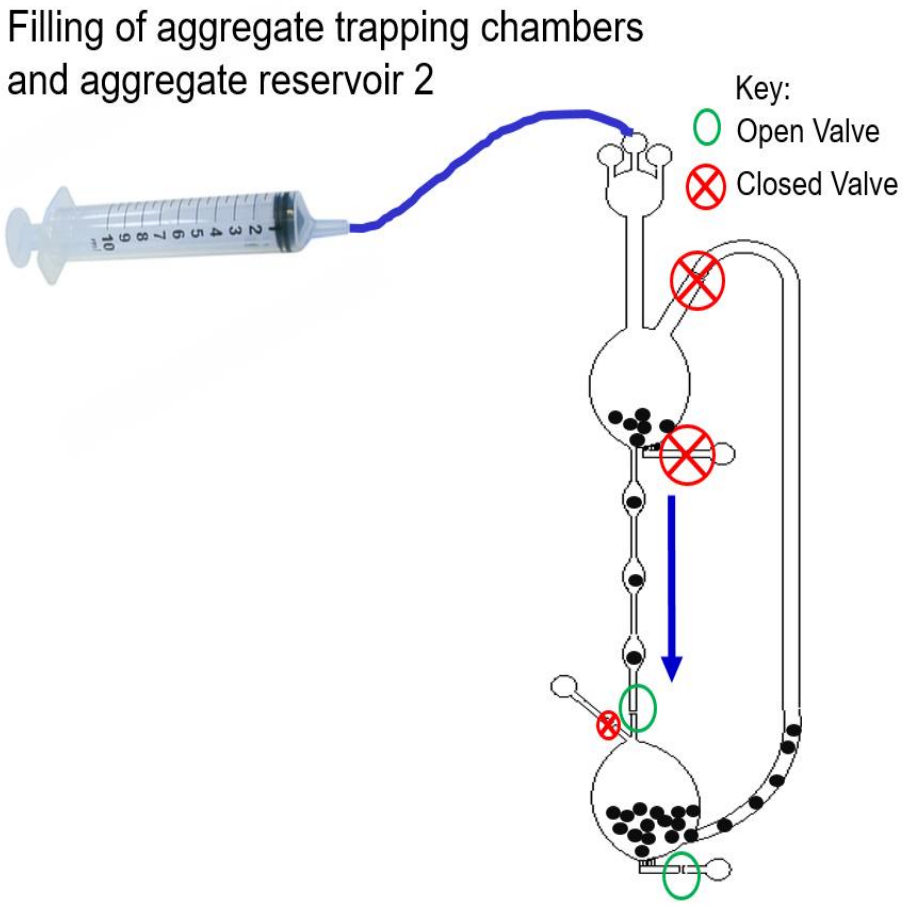

Figure 15: Step 2 is the aggregate trapping process

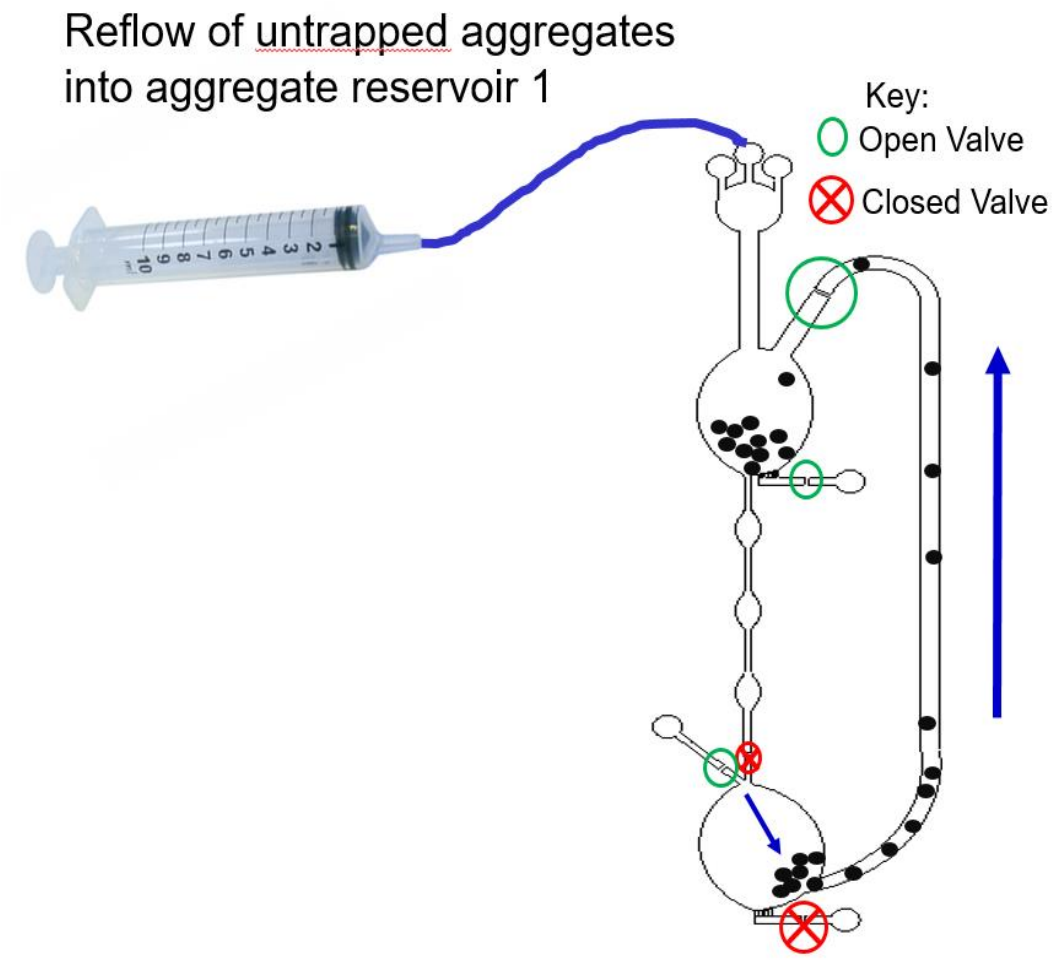

Figure 16: Step 3 is the reflow of remaining aggregates through the trapping structures

The reflow of the neuronal aggregates depicted in Figures 14-16 recirculates the un-trapped aggregates. This allows filling of any unfilled aggregate traps and minimizes the loss of previously un-trapped aggregates.

2.2 Trapping Structures

In addition to the above microfluidic design, the previously designed trapping structure was analyzed. The trap design was tested using COMSOL simulations and

fabrication was attempted using DRIE. The previously designed structure consisted of three pillars spaced approximately 35 um apart. The aspect ratio of these pillars approached 6. This proved difficult to fabricate using traditional SU-8 techniques. Therefore, fabrication was attempted using DRIE. Multiple potentially viable trapping structures were designed as alternatives to the previous trapping structure to potentially improve the fabrication process. The goal was to reduce the difficulty of the fabrication process for the neuronal aggregate traps. The size of the traps as well as the shape of the traps was altered in an attempt to accommodate the fabrication process.

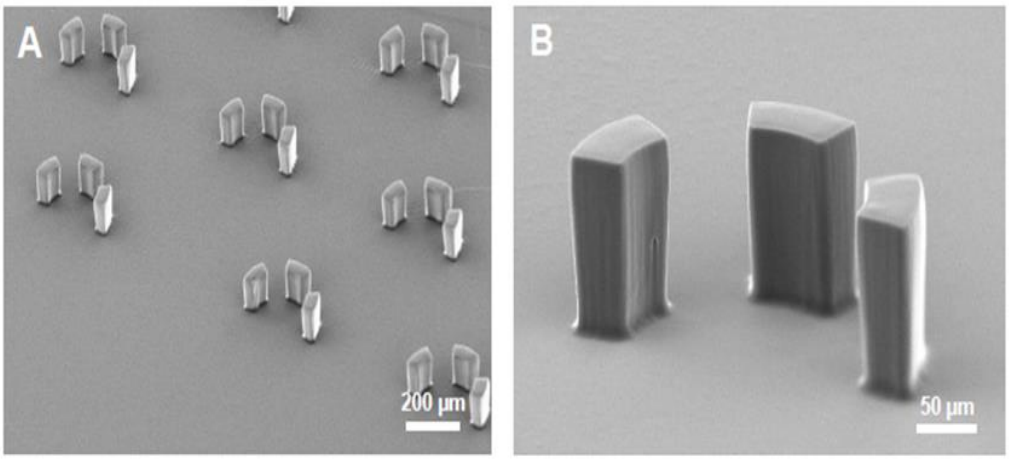

Figure 17: Microfabricated trapping pillars [3]

Comsol simulations were run for each of the trapping structures, including those shown in Figure 17, to measure the flow velocity around each of the trapping structures. A higher flow velocity is depicted in red and provides the most likely path for fluid to

flow. The traps were design to have high flow through the center of the trapping structures to increase the likelihood of trapping an aggregate. In the previous trapping structure a higher flow rate between the two trapping pillars allowed for fluid to flow into the trapping region. This high flow rate between the pillars of the trapping structure, seen in Figures 18 and 19, was mimicked in the new designs.

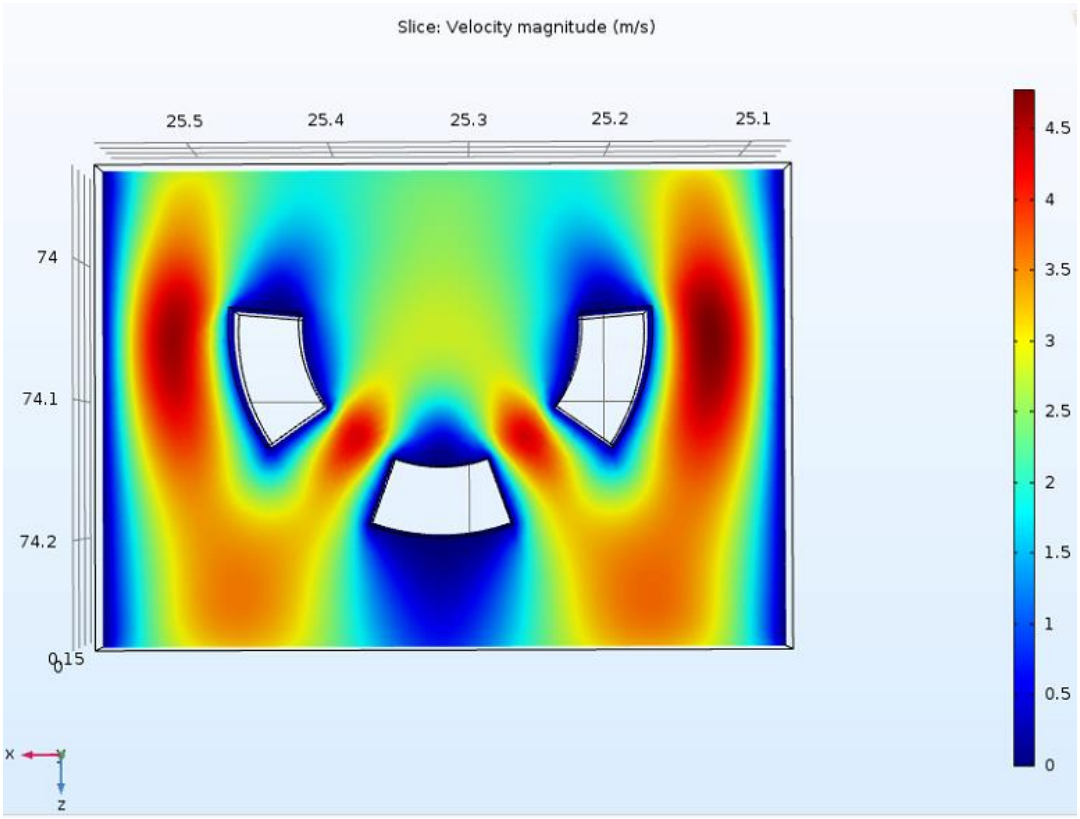

Figure 18: Comsol simulation of previous aggregate trapping design.

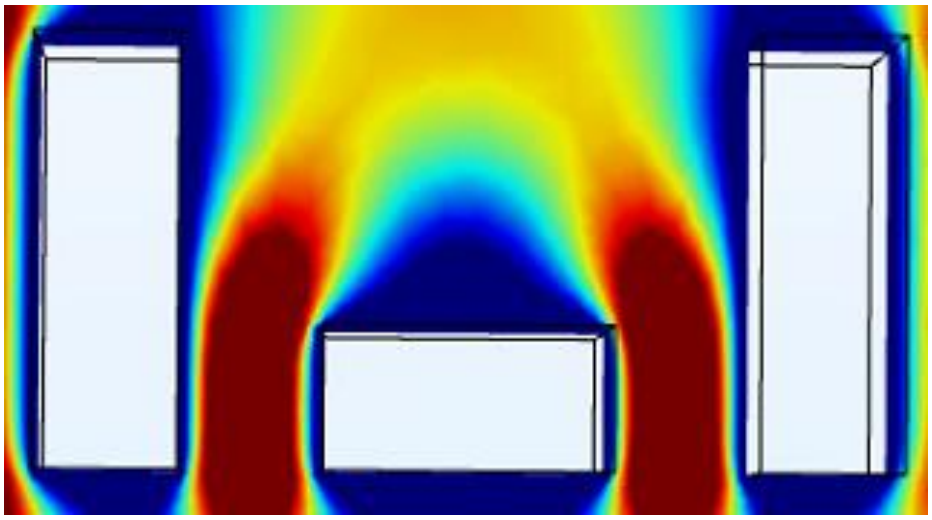

Figure 19: Comsol simulation of new block trapping structure.

The block pillar structures increased the size of the aggregate trap width by approximately 35 percent from 37 um to 50 um. Also, the length of the traps increased to approximately double. The space between the adjacent pillars was set at 50 um. A larger gap may allow the aggregates to pass though the two pillars. The distance between the two large pillars is 200 um, the size of the aggregates. Increasing the size of the structure as well as the gap should increase the ease of fabrication. A simulation combining multiple trapping structures is shown in Figure 20.

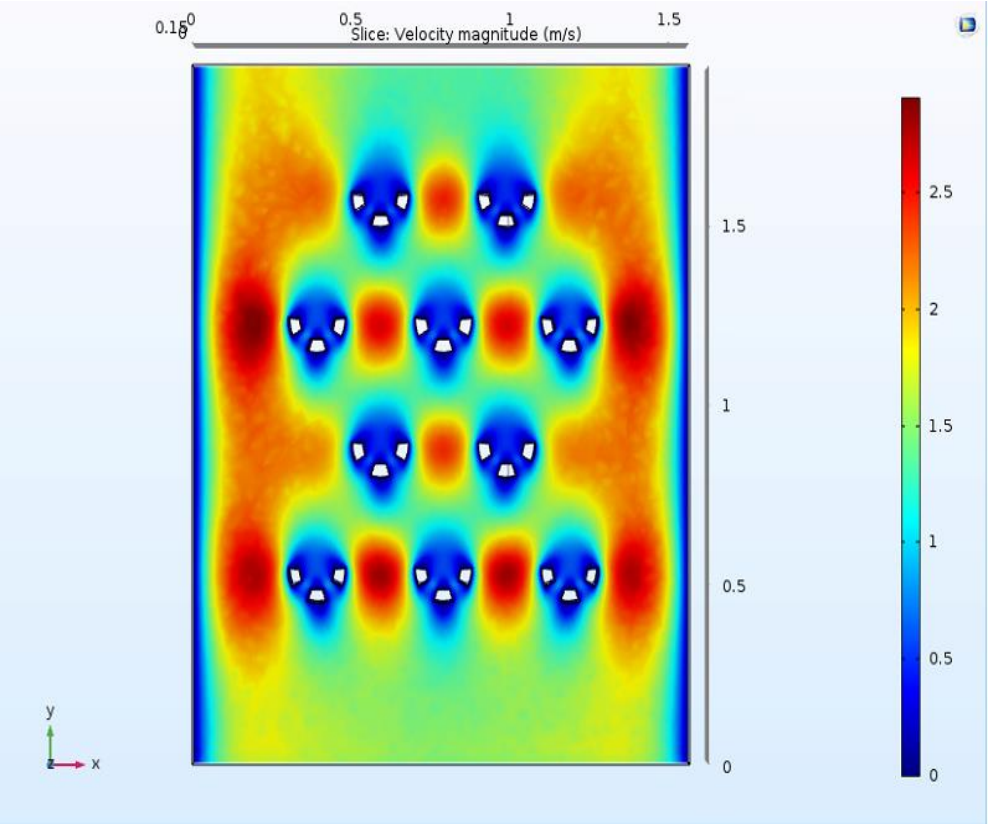

Figure 20: Comsol simulation of previous trapping structure.

2.3 Fabrication of Neuronal Aggregate Device

SU-8 photoresist was patterned on 3'' inch silicon wafers to form the molds for the PDMS channel and valve layers. The SU-8 was spin coated onto the wafers at 1000 rpm for 1 min to obtain 200 um thickness. Next, the spin coated wafers were soft baked at 65C for over 24 hours. The wafers were hard baked at 95C for 40 minutes prior to UV exposure. The Karl Suss MA6 mask aligner in Aggiefab was used to expose the hard baked wafers to UV light. An intensity of 300mJ/cm^2 was obtained to properly pattern the wafers. Post exposure baking was performed at 95C for 20 minutes. The wafers were

then developed using SU-8 developer for approximately 15 minutes. After developing the patterned wafers were rinsed using first IPA then DI water. Following developing, the wafers were air dried with nitrogen and coated with trichlorosilane. Evaporation of the trichlorosilane onto the wafers was performed in a vacuum chamber for 20 minutes. Once coated with trichlorosilane, the molds were ready for curing with PDMS.

Silicon elastomer 184 was the base PDMS polymer. It was mixed in a 10:1 ratio with curing agent to form the PDMS pre polymer. After thorough mixing, the mixture of base polymer and curing agent was degassed in a vacuum chamber. This degassing formed the PDMS pre polymer. The pre polymer was poured onto the SU-8 molds. To harden the PDMS, the degassed mixture was placed in a drying oven for over 40 minutes. Once hardened, the cured PDMS could be cut out from the SU-8 molds. The cut out PDMS contained valve channels corresponding to the areas of hardened SU-8 photoresist on the wafer. An overview of the fabrication procedure is shown in Figure 21.

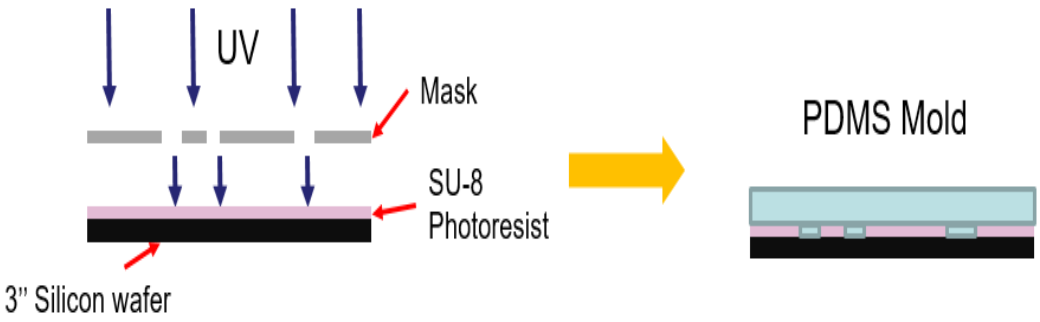

Figure 21: Fabrication process using SU-8 photoresist

To obtain the channel layer, a slightly different approach was employed. The channel layer needs to be thin for the valves to work properly. In order to obtain a thin channel layer, PDMS pre polymer was spin coated onto the SU-8 channel mold at 300 rpm for 40 seconds. This obtained the proper thickness of 300 um. The spin coated wafer needs to be cured for at least 6-8 hours before removing the thin membrane. Attempting to remove the membrane without sufficient curing time led to distortion of features in the channel layer.

After curing of the channel and valve layers, they were removed from the SU-8 molds. The top of the channel layer was bonded to the valve layer. The bonding process involved plasma treating the top channel layer and the bottom of the valve layer. The plasma treatment results in oxygen bonding to the surface of the PDMS. The oxygen saturated surfaces of the top of the channel layer and the bottom of the valve layer bond to each other. Aligning the channel layer with the valve layer required use of a special bonding technique following plasma treatment. Immediately following plasma treatment, the valve layer was placed on a hotplate at 150C. The valve layer was sprayed with methanol to prevent the channel layer from immediately bonding to the valve layer. This allowed for time to align the two layers. The methanol begin to evaporate immediately at a high temperature only allowing for a short time period for alignment. The bonding need to occur within 4 minutes for a good bond to occur between the two PDMS layers. After spraying the valve layer with methanol, the plasma treated side of the channel layer is aligned with the valve layer. Once alignment is finished, the remaining methanol evaporates and the two PDMS layers come into contact resulting in

bonding. The recently bonded PDMS layers are placed in a curing oven at 85C for 24 hours. Baking in a curing oven removes remaining hydrophilicity in the channel layers preventing sticking of the channel to the valve layer in the next step.

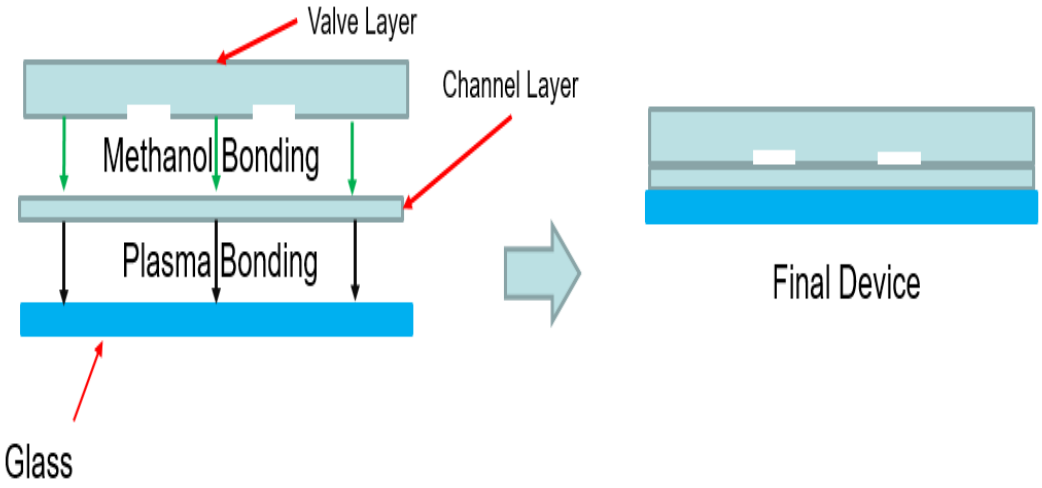

Figure 22: Fabrication of recirculation device

After 24 hours in a curing oven, the next plasma bonding step is introduced and is depicted in Figure 22. The bonded valve and channel layers are plasma treated along with a glass slide. Immediately following plasma treatment, the valves are actuated using 10 mL syringes. This applies negative pressure to the valve layer and suck the channel wall below the valves up, essentially opening the channel. Sucking the channel layer below the valves up prevents it from sticking to the glass slide. After all the valves are actuated, the channel layer is bonded to the plasma treated side of the glass slide. It is

allowed to bond for at least 15 minutes. Time is given for the hydrophilicity of the glass to reduce so that the glass does not bond to the channel layer when the valves are closed.

2.4 Fabrication of Trapping Structures

Initially, the fabrication of the trapping structures was performed using traditional SU-8 techniques as previously described. SU-8 was spin coated onto silicon wafers and exposed to UV light to form a master mold. Following SU-8 fabrication, Inductively Coupled Reactive Ion Etching (ICP-RIE) was used to etch silicon.

ICP-RIE was performed using Oxford Plasmalab 100 ICP-RIE system in Aggiefab. A 2000A layer of chrome was deposited on the surface of the silicon wafer and spin coated with photoresist. Following soft bake, the photoresist was patterned using UV light and developed. After developing, shown in Figure 23, the wafer was hard baked at 80 C for 10 minutes.

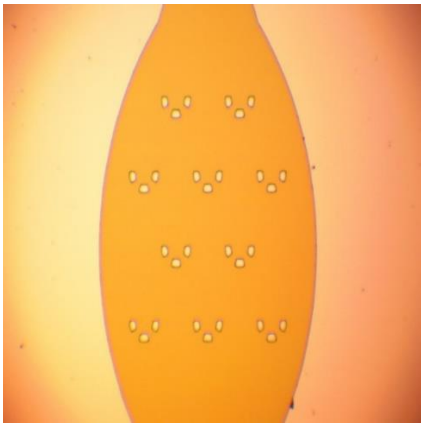

Figure 23: After developing step

The wafer was then etched in chrome etchant as shown in Figure 24. The photoresist was then removed using a wash of first Isopropyl alcohol and then acetone. Any remaining photoresist was removed with cotton swabs soaked in acetone. The final step result is shown in Figure 25.

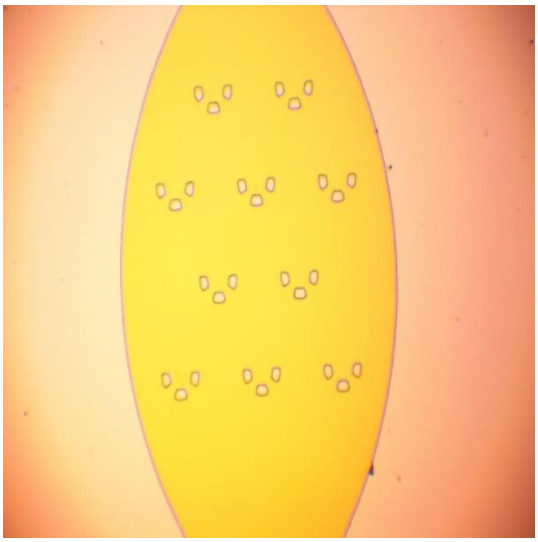

Figure 24: After chrome etch

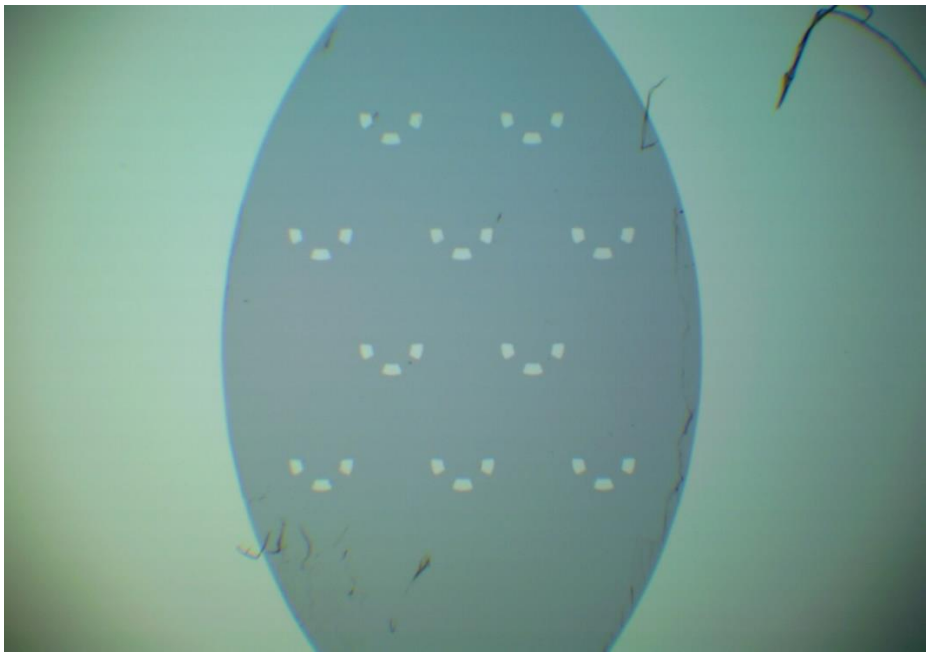

Figure 25: After PR strip.

CHAPTER III

RESULTS AND DISCUSSION

3.1 Recirculation Device Characterization

Polystyrene beads with 175 um diameter were flown through the recirculation device to test correct valve operation. The beads were successfully circulated throughout the device. They were loaded into reservoir 1 and flown through the aggregate trapping chambers. After loading into reservoir 2, they were recirculated back into reservoir 1. The process was repeated and the beads were successfully recirculated throughout the device. Some issues with polystyrene beads include sticking of the beads to PDMS substrate. This resulted in some of the beads sticking to the PDMS channel. In order to avoid this issue, a very high flow rate was used. Manual loading of the beads with a syringe required a much higher flow rate than with traditional cell aggregates.

After verification of the design concept with polystyrene beads, actual cell aggregates were loaded onto the microfluidic device. A HeLa cell line was used in the formation of the cell aggregates. This was done in lieu of neuronal aggregate cells due to the lack of neuronal cells. HeLa cells form good aggregates and are relatively easy to culture. The cell aggregates were formed by seeding the cell aggregates onto PDMS microwells. The cells were cultured on these microwells for up to one week to form tight aggregates. The aggregates were removed from the microwells and flown through the PDMS device. The loading of the aggregates was performed at a much slower flow rate than the polystyrene beads. The aggregates were flown into the device at a rate ranging

from 300 – 800 ul/min. This lower flow rate preserved the structure of the aggregates by preventing them from breaking apart. The size of the aggregates varied widely from 50 to 150 um size. This non uniform size was due primarily to the lack of culture time in the microwells. In following experiments, the aggregates will be cultured for a period of two weeks or until tight spheroid formation is seen in the microwells. Furthermore, a low concentration of aggregates was used due to the lack of large aggregates of the size 150 um or greater. Despite these drawbacks, basic functioning of the device was shown and the aggregates were circulated through the device. In future work, uniform cell aggregates will be cultured to further test the capabilities of the design. Different cell aggregates including both neuronal cells and HeLa cells will be cultured.

3.2 Aggregate Trap Fabrication

The fabrication of the pillar structures using SU-8 was unsuccessful due to peeling of SU-8 from the master mold during removal of the PDMS. This resulted from the high aspect ratio of the pillar structures shown in Figure 27. In addition to the peeling of the SU-8, the resulting pillars were connected as shown in Figures 26 and 28. This prevented flow between the pillars. Removal of the chrome from the silicon was an issue as depicted in Figure 29.

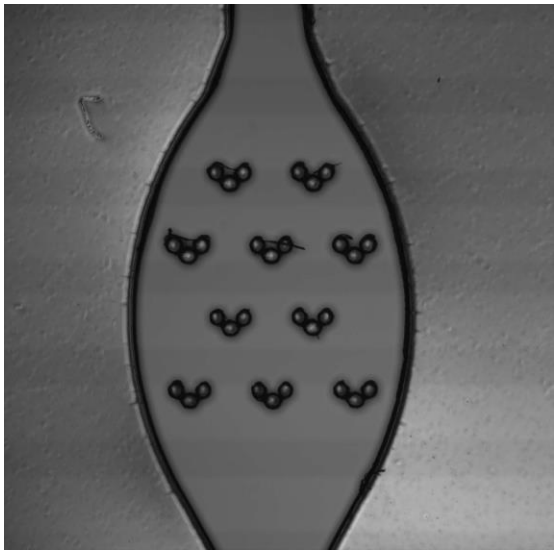

Figure 26: SU-8 pillar structure exposed at 270 mJ/cm^2 UV intensity

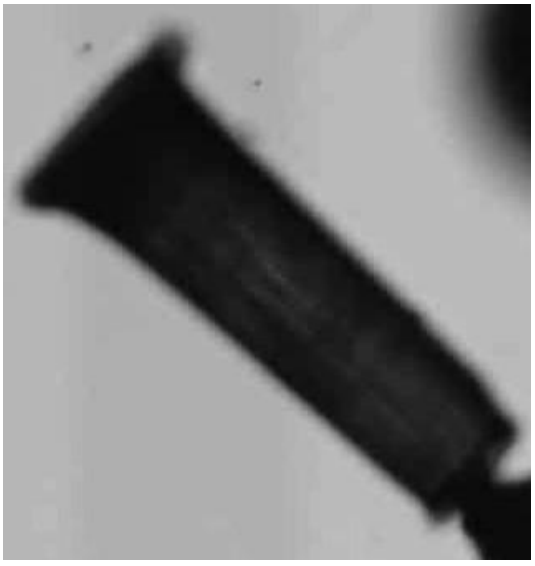

Figure 27: Sideview of pillar structure

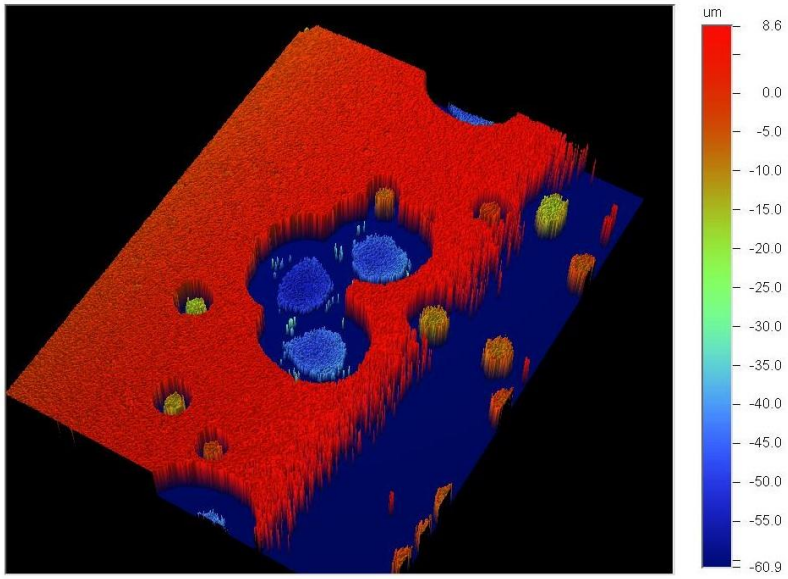

Figure 28: 3D plot of etched trapping structure.

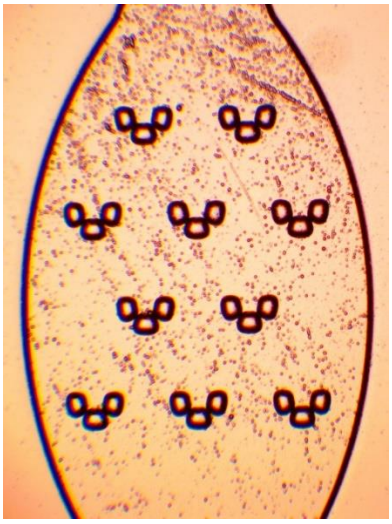

Figure 29: Chrome mask removed from etched silicon wafer.

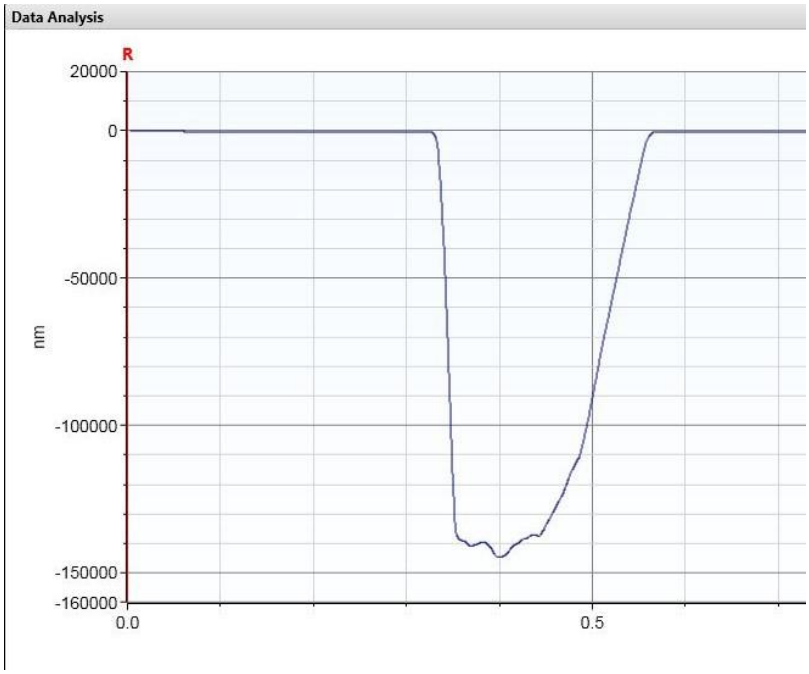

Figure 30: Depth profile of block structure.

Previously a master mold for the aggregate traps was fabricated in a DRIE in Korea. This was due to the high aspect ratio of the pillars. The attempts to increase the size and reduce the aspect ratio of the trapping structures were a step towards successful fabrication. Further etching tests need to be performed to determine the maximum distance needed to correctly resolve two aggregate trapping pillars.

An etching depth of up to 150 um was achieved and is shown in Figure 30. This is sufficient for an aggregate size of 150 – 200um. However, the sidewall passivation resulted in merging of the pillar structures and further research into the proper distance between etched structures is required. Altering the ratio of SF_6 gas to O_2 should change the sidewall characteristics of the etch. Increasing the amount of O_2 should increase

sidewall passivation thus resulting in a straighter sidewall. The downside to increased O_2 passivation is the reduced silicon etch rate. A faster etch rate is important when considering the depth of the etch is 200 um. Various ratios of SF_6 to O_2 were attempted and compared in Table 1.

	SF_6	**O_2**	**RF Power**	**ICP Power**	**Chamber Pressure**	**Temp**
Oxford Recipe	70 sccm	4.5 sccm	5W	900W	10 mTorr	-100 C
Song Recipe	70 sccm	20 sccm	20W	900W	10 mTorr	-100 C
Previous Recipe (Akil 45 min etch)	90 sccm	30 sccm	10W	900W	15 mTorr	-100 C
Han's Recipe	70 sccm	4.0 sccm	60W	900W	10mTorr	-100 C
Arif Modified Recipe	90 sccm	30 sccm	30W	900W	15mTorr	-100 C

Table 1: List of etching recipes

Width of Trench	Si etch rate
50 um	2.08 um/min
800 um	8.3 um/min

Table 2: Etching rate for Akil 45 min etch

Width of Trench	Si etch rate
50 um	2 um/min
800 um	3 um/min

Table 3: Etch rate using Oxford recipe

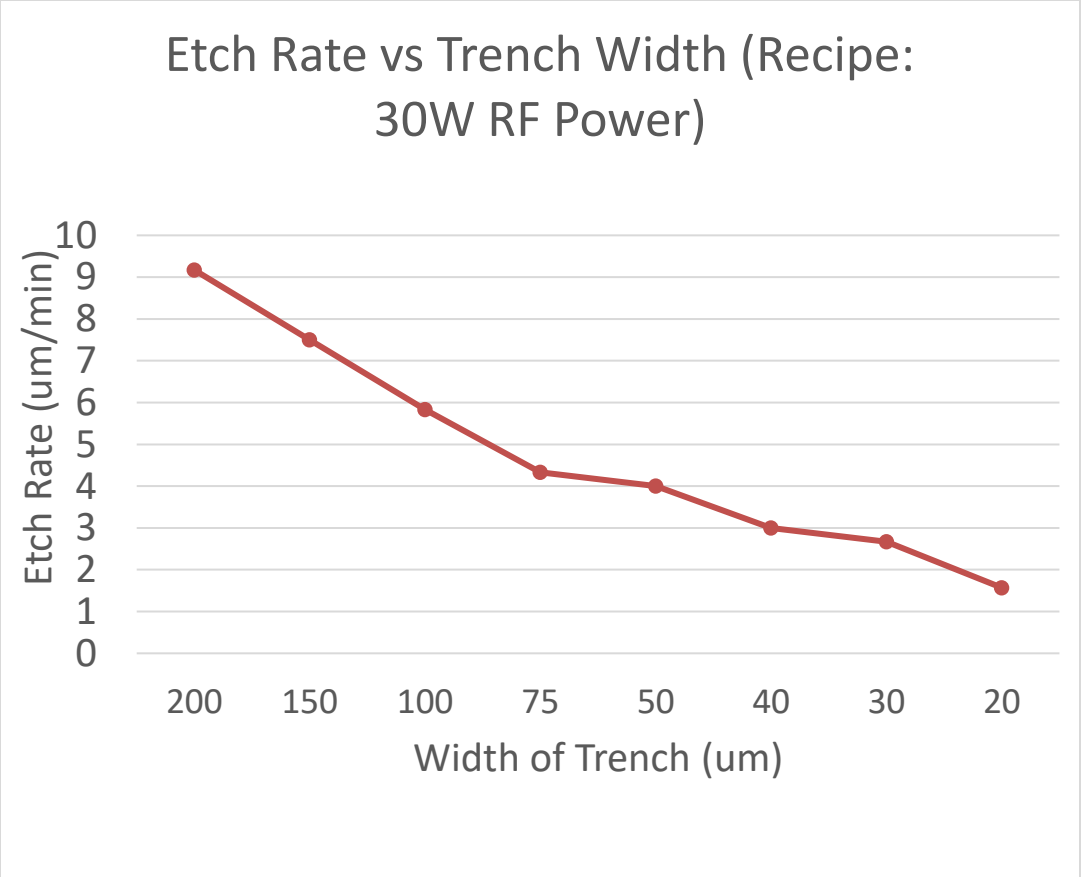

Figure 31: Etch rate vs trench width

The recipes showing the deepest etch down to 150 um were Akil's 45 minute etch, shown in Table 2, and Oxford's recipe, shown in Table 3. Despite having an increased oxygen flow rate, Akil's 45 minute etch achieved the same etch rate for a 50 um width trench as Oxford's recipe due to increased RF power. These recipes achieved similar etch depths as well as sidewall profiles. This is interesting due to the difference in the ratios between SF_6 and O_2. In general, as the width of the trench increased, the etch rates decreased as shown in Figure 31.

CHAPTER IV

SUMMARY AND FUTURE WORK

4.1 Effect of Recirculation of Aggregates

A microfluidic device was successfully designed, fabricated and tested for the recirculation of cellular aggregates. This device enables reflow of cellular aggregates within a microfluidic platform. The wide ranging implications of such a device include the recirculation of neuronal aggregates through aggregate trapping structures. This will limit neuronal aggregate loss reducing the cost of myelination studies. This impacts the previous research performed on the myelination of neuronal aggregates increasing the efficiency of myelination studies. Furthermore, the recirculation design provides the potential for a high throughput design. The design will be increased to contain up to 48 aggregate trapping chambers. An inlet and outlet for each row of aggregate trapping chambers will be included along with more mircovalves to control the flow of media into and out of the chambers. This will allow parallel testing of different drug compounds or different concentrations of drugs within each row of aggregate culturing chambers. Continued testing with different cell aggregates will be done including tests with neuronal aggregates. Uniform aggregates will be culturing within microwells and circulated through the trapping chambers. The fabrication of a recirculation design that includes the aggregate trapping pillars is necessary for continued research into the trapping efficiency. Incorporation of the trapping pillars into the design is discussed in the following section.

4.2 Aggregate Traps

Fabrication of the aggregate trapping pillars will continue to be tested within Texas A&M's Aggiefab. Increasing the size of the pillars as well as the distance between the pillars may help in the fabrication process. Etching of trenches into silicon with the tools availbale at Texas A&M has shown the capabilities to etch structures as deep as 150 um. If the size of the trapping structures is increased significantly then it is possible to fabricate the structures using SU-8 photoresist without the detrimental peeling effect. If unsuccessful in fabrication of the trapping pillars using currently available techniques, the device will be fabricated by a professional DRIE lab.

REFERENCES

[1] Dupin, I., M. Dahan, and V. Studer. "Investigating Axonal Guidance with Microdevice-Based Approaches." Journal of Neuroscience 33.45 (2013): 17647-7655.

[2] El-Ali, Jamil, Peter K. Sorger, and Klavs F. Jensen. "Cells on Chips." Nature 442 (2006): 403-11. Print.

[3] Park, Jaewon. "Microsystems for in vitro CNS neuron study." Diss. Texas A&M U, 2011. Print.

[4] Podbielska, Maria, Naren Banik, Ewa Kurowska, and Edward Hogan. "Myelin Recovery in Multiple Sclerosis: The Challenge of Remyelination." *Brain Sciences* 3.3 (2013): 1282-324. Web.

[5] Ihara, Masafumi, Tuomo M. Polvikoski, Ros Hall, Janet Y. Slade, Robert H. Perry, Arthur E. Oakley, Elisabet Englund, John T. O'Brien, Paul G. Ince, and Raj N. Kalaria. "Quantification of Myelin Loss in Frontal Lobe White Matter in Vascular Dementia, Alzheimer Disease, and Dementia with Lewy Bodies." Acta Neuropathologica 119.5 (2010): 579-89.

[6] Sherman, Diane L., and Peter J. Brophy. "Mechanisms of Axon Ensheathment and Myelin Growth." Nature Reviews Neuroscience 6.9 (2005): 683-90.

[7] Lindner, Maren, Katja Thammler, Ariel Arthur, Sarah Brunner, Christina Elliott, Daniel Mcelroy, Hema Mohan, Anna Williams, Julia M. Edgar, Cornelia Schuh, Christine Stadelmann, Susan C. Barnett, Hans Lassmann, Steve Macklisch, Manikhandan Mudaliar, Nicole Schaeren-Wiemers, Edgar Meinl, and Christopher

Linington. "Fibroblast Growth Factor Signalling in Multiple Sclerosis: Inhibition of Myelination and Induction of Pro-inflammatory Environment by FGF9." Brain 138.7 (2015): 1875-893.

[8] Ponath, Gerald, Sriram Ramanan, Mayyan Mubarak, William Housley, Seunghoon Lee, F. Rezan Sahinkaya, Alexander Vortmeyer, Cedric S. Raine, and David Pitt. "Myelin Phagocytosis by Astrocytes after Myelin Damage Promotes Lesion Pathology." Brain 140.2 (2016): 399-413.

[9] "Fingolimod: Indications, Side Effects, Warnings." Drugs.com. Drugs.com, Web. 08 Feb. 2017.

[10] Mueller, Bernhard K., Helmut Mack, and Nicole Teusch. "Rho Kinase, a Promising Drug Target for Neurological Disorders." Nature Reviews Drug Discovery 4.5 (2005): 387-98.

[11] Schneider, L. S., F. Mangialasche, N. Andreasen, H. Feldman, E. Giacobini, R. Jones, V. Mantua, P. Mecocci, L. Pani, B. Winblad, and M. Kivipelto. "Clinical Trials and Late-stage Drug Development for Alzheimer's Disease: An Appraisal from 1984 to 2014." Journal of Internal Medicine 275.3 (2014): 251-83.

[12] Avorn, Jerry. "The $2.6 Billion Pill" Methodologic and Policy Considerations." New England Journal of Medicine 372.20 (2015): 1877-879.

[13] Blasiak, Agata, Hae Ung Lee, Sudip Nag, and In Hong Yang. "Compartmentalized Microfluidic Platform Integrated with Subcellular Electrical Stimulation for Studying Activity-dependent Axon Myelination." 2016 International Conference on Optical MEMS and Nanophotonics (OMN) (2016).

[14] Yang, In Hong, Rezina Siddique, Suneil Hosmane, Nitish Thakor, and Ahmet Hake. "Compartmentalized Microfluidic Culture Platform to Study Mechanism of Paclitaxel-induced Axonal Degeneration." Experimental Neurology 218.1 (2009): 124-28.

[15] Hur, E.-M., I. H. Yang, D.-H. Kim, J. Byun, Saijilafu, W.-L. Xu, P. R. Nicovich, R. Cheong, A. Levchenko, N. Thakor, and F.-Q. Zhou. "Engineering Neuronal Growth Cones to Promote Axon Regeneration over Inhibitory Molecules." Proceedings of the National Academy of Sciences 108.12 (2011): 5057-062.

[16] Morin, Fabrice, Naoki Nishimura, Laurent Griscom, Bruno Lepioufle, Hiroyuki Fujita, Yuzuru Takamura, and Eiichi Tamiya. "Constraining the Connectivity of Neuronal Networks Cultured on Microelectrode Arrays with Microfluidic Techniques: A Step towards Neuron-based Functional Chips." Biosensors and Bioelectronics 21.7 (2006): 1093-100.

[17] Park, Jeong Won, Behrad Vahidi, Anne M. Taylor, Seog Woo Rhee, and Noo Li Jeon. "Microfluidic Culture Platform for Neuroscience Research." Nature Protocols 1.4 (2006): 2128-136.

[18] Yap, Yiing C., Tracey C. Dickson, Anna E. King, Michael C. Breadmore, and Rosanne M. Guijt. "Microfluidic Culture Platform for Studying Neuronal Response to Mild to Very Mild Axonal Stretch Injury." Biomicrofluidics 8.4 (2014): 044110.

[19] Peyrin, Jean-Michel, Barangare Deleglise, Laure Saias, Maava Vignes, Paul Gougis, Sebastien Magnifico, Sandrine Betuing, Mathaa Pietri, Jocelyne Caboche, Peter Vanhoutte, Jean-Louis Viovy, and Bernard Brugg. "Axon Diodes for the Reconstruction

of Oriented Neuronal Networks in Microfluidic Chambers." Lab on a Chip 11.21 (2011): 3663.

[20] Hallfors, Nicholas, Asif Khan, Michael D. Dickey, and Anne Marion Taylor. "Integration of Pre-aligned Liquid Metal Electrodes for Neural Stimulation within a User-friendly Microfluidic Platform." Lab Chip 13.4 (2013): 522-26.

[21] Benfenati, Valentina, Stefano Toffanin, Simone Bonetti, Guido Turatti, Assunta Pistone, Michela Chiappalone, Anna Sagnella, Andrea Stefani, Gianluca Generali, Giampiero Ruani, Davide Saguatti, Roberto Zamboni, and Michele Muccini. "A Transparent Organic Transistor Structure for Bidirectional Stimulation and Recording of Primary neurons." Nature Materials 12.7 (2013): 672-80.

[22] Mehling, Matthias, and Sava Tay. "Microfluidic Cell Culture." Current Opinion in Biotechnology 25 (2014): 95-102.

[23] Melin, Jessica, and Stephen R. Quake. "Microfluidic Large-Scale Integration: The Evolution of Design Rules for Biological Automation." Annual Review of Biophysics and Biomolecular Structure 36.1 (2007): 213-31.

[24] Halldorsson, Skarphedinn, Edinson Lucumi, Rafael Gomez-Saberg, and Ronan M.T. Fleming. "Advantages and Challenges of Microfluidic Cell Culture in Polydimethylsiloxane Devices." Biosensors and Bioelectronics 63 (2015): 218-31.

[25] Park, Jaewon, Hisami Koito, Jianrong Li, and Arum Han. "Microfluidic Compartmentalized Co-culture Platform for CNS Axon Myelination Research." Biomedical Microdevices 11.6 (2009): 1145-153.

[26] Mohan, Ritika, Benjamin R. Schudel, Amit V. Desai, Joshua D. Yearsley, Christopher A. Apblett, and Paul J.A. Kenis. "Design Considerations for Elastomeric Normally Closed Microfluidic Valves." Sensors and Actuators B: Chemical 160.1 (2011): 1216-223.

[27] Araci, Ismail Emre, and Philip Brisk. "Recent Developments in Microfluidic Large Scale Integration." Current Opinion in Biotechnology 25 (2014): 60-68.

[28] Carlo, Dino Di, Liz Y. Wu, and Luke P. Lee. "Dynamic Single Cell Culture Array." Lab on a Chip 6.11 (2006): 1445.

[29] Nilsson, J., M. Evander, B. Hammarstram, and T. Laurell. "Review of Cell and Particle Trapping in Microfluidic Systems." Analytica Chimica Acta 649.2 (2009): 141-157.